BIW10 Preprint -- Edited; preliminary green dot status
Final version will appear on JACoW

BEAM LOSS MONITORS (BLMS): PHYSICS, SIMULATIONS AND APPLICATIONS IN ACCELERATORS

A. Zhukov, ORNL, Oak Ridge, TN, U.S.A.

Abstract

Beam loss monitors are common devices used in hadron and lepton accelerators. Depending on accelerator specifics, BLMs could be just diagnostics or could play an essential role in the machine protection system (MPS). This tutorial discusses different types of BLMs and their applicability to different accelerators. It covers traditional BLMs like ionization chambers and scintillator-based devices, and also less common techniques like those based on fiber optics and avalanche diodes. The tutorial gives an overview of the underlying physics involved in beam loss detection, and recent advances in computer simulation of particle interaction with matter helpful for BLM modeling. Options for signal processing electronics are described, as well as interfaces to both the control system and the MPS.

INTRODUCTION

Definition

First we want to define a beam loss and a beam loss monitor. Charged particles are accelerated in accelerators and supposed to follow design trajectory along the beam line. Some of the particles deviate from the prescribed path and hit the beam pipe. They then interact with media and create radiation. So the beam loss is *unintentional* interaction of beam particles with media causing radiation. A beam loss monitor is intended to detect this radiation. Sometimes the particles interact with materials by design; good examples of that are Faraday cups, wire scanners, collimators, scrapers and other insertable devices. The presence of such devices complicates analysis of BLM signals since they add significantly to radiation field around them. In addition, there are other sources of radiation that do not involve direct interaction of primary particles with materials. These sources include synchrotron radiation and cavity X-rays. An ideal BLM should be sensitive to radiation caused by loss and insensitive to other sources of radiation. While one can imagine a beam loss detector that is not a radiation detector we won't discuss such devices in this paper.

BLM Purpose

The ultimate goal of a BLM system is to identify the loss level and if possible, the loss's location and time structure. This could result in a beam abort if the loss level endangers equipment (for example, by burning a hole in a drift tube or quenching a superconducting magnet). It also can provide feedback for better beam tuning. Residual activation is a big problem for high power hadron machines; the BLMs can help to limit that.

General BLM-specific considerations

While beam loss monitors are commonly used as beam diagnostics devices, beam loss is a somewhat standalone topic of beam instrumentation. This is probably due to the nature of the physics processes the BLMs rely on. Other diagnostics devices usually are directly coupled with Accelerator physics and electrodynamics principles. BLMs involve many different parts of physical science, such as: electrodynamics, high-energy particle detectors, nuclear physics, radiation protection, neutron physics, etc. Due to this fact, beam diagnostics overview papers typically mention the physics processes inside BLMs briefly and interpret a BLM as a black box with known parameters and detector response function. We will try to give an overview of radiation detector physics here and refer to corresponding literature for more in-depth information [1,2,3].

The other important fact to consider is the sensitivity of loss monitors to real world geometry. Usually, a BLM is a radiation detector which is placed in an accelerator tunnel in the vicinity of the beam pipe; almost everything that is located nearby could potentially influence the BLM by attenuating (or in some cases increasing) the radiation field measured by the detector. This fact makes detailed analytic calculations of losses almost impossible in any non-ideal case. Fortunately many computer codes exist to address this problem. These codes account for both the vast distribution of involved physics and the complex physical layout of modern accelerators.

BLM PHYSICS ASPECTS

Electromagnetic interaction of charged particles with a medium

As we will see later the interaction of charged particles with materials is the most important thing to consider while designing a BLM. When a charged particle passes through matter, it loses its energy by ionization and atomic excitation. These processes are dictated by the EM interaction between atomic electron and incident charged particle.

The Bethe-Bloch equation is the main formula governing this process:

$$-\frac{dE}{dx} = 0.31\,\frac{MeV}{g/cm^3}\,z^2\,\frac{Z}{A}\,\frac{1}{\beta^2}\left(\ln\frac{2m_e c^2\gamma^2\beta^2}{I} - \beta^2 - \frac{\delta}{2}\right), \quad (1)$$

where Z/A is the ratio of atomic charge and the atomic mass number, z is the charge of the incident particle (in units of electron charge), m_e is the electron's rest mass and I is the ionization potential – a property of the atom; all other variables denote standard relativistic quantities.

This formula gives the average energy loss (*stopping power*) of a heavy particle (not an electron or positron) per unit of length (expressed in g/cm^3 to account for the fact that the probability of interaction is proportional to atom concentration; to obtain energy loss per cm one should multiply (1) by the material density in g/cm^3). Simple relativistic kinematics [4] shows that the numerator of the logarithmic term is a maximum of energy transferrable to the released electron. The energy loss of a proton in nitrogen is shown in Fig. 1.

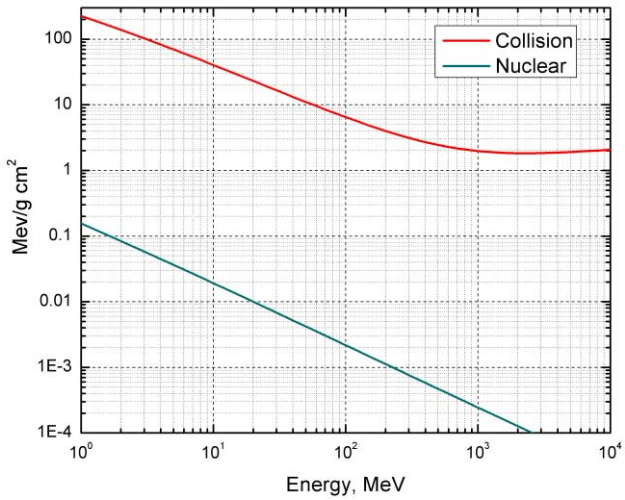

Figure 1: Stopping power for proton in nitrogen. NIST data [5].

In order to obtain the formula for electrons one has to consider the mass equality of the incident particle and the released electron; also, there is no way to distinguish between incident electrons and shell electrons after a collision. This gives a different maximum energy transfer for a relativistic electron [4].

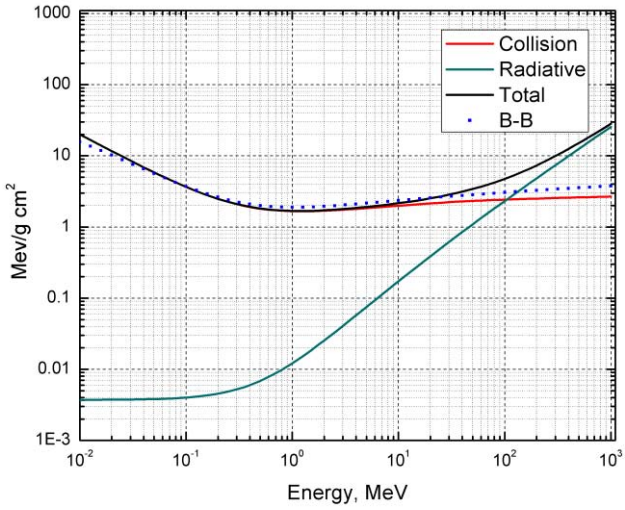

Figure 2: Stopping power for electrons in nitrogen, NIST data [5] and Bethe-Bloch (B-B) evaluation.

For this and other reasons (discussed later), the stopping power curve looks different for electrons, as shown in Fig. 2. This curve is given by a modified Bethe-Bloch equation:

$$-\frac{dE}{dx} = 0.31\,\frac{MeV}{g/cm^3}\,\frac{Z}{A}\,\frac{1}{\beta^2}\left(\ln\frac{m_e c^2\gamma}{2I} - \beta^2 - \frac{\delta}{2}\right). \qquad (2)$$

Since Eqns. (1) and (2) define average loss, it is important to understand the size of the fluctuations of this value. It is parameterized by a Landau distribution [4], but the actual distribution could be even wider. Also, the particles are subject to *range straggling*, caused by fluctuations in path lengths of particles having the same initial energy. For heavy particles it range varies within several percents. This explains different shapes for the curves of stopping power vs. penetration depth (the Bragg peak for heavy particles and lack of it for electrons).

Electrons also experience bremsstrahlung due to Coulomb interaction with the atomic nucleus and at some energy the collisional loss is equal to the radiative loss. Classical electrodynamics theory gives

$$-\left(\frac{dE}{dx}\right)_{rad} \approx \frac{Z^2}{A}\,\frac{1}{m^2c^4}\,E\ln\frac{183}{Z^{1/3}}, \qquad (3)$$

where the square of particle mass in the denominator reflects the fact that radiative loss is negligible for heavy particles.

The ratio of collisional and radiative loss is given by (energy in MeV):

$$-\frac{(dE/dx)_{rad}}{(dE/dx)_{col}} \cong \frac{EZ}{700}. \qquad (4)$$

Since the radiative loss is proportional to energy, it is useful to introduce the parameter X_0 – radiation length. We can then write (3) in common exponential attenuation form:

$$-\left(\frac{dE}{dx}\right)_{rad} = \frac{E}{X_0} \qquad (5)$$

Equations 1-5 allow estimating the scale of energy loss by charged particles inside a BLM detector volume.

Gamma and X-ray interactions

While gamma particles could not be primary particles for an accelerator, they are always present as secondaries. They participate in three interactions:

- Photoelectric absorption (dominant for low energies: ~30 keV).
- Compton scattering (100 keV~2 MeV).
- Pair production.

During photoelectric absorption, a photon interacts with the whole atom and kicks out an electron. Usually (with about 80% probability) the absorption happens in a K shell. The photoelectric cross section is proportional to Z^5. The Born approximation [6] of Eqn. (4) gives a good

description for K-shell absorption in the non-relativistic case:

$$\sigma_{photo}^{K} = \left(\frac{32}{\varepsilon^{7}}\right)^{1/2} Z^{5} \alpha^{4} \sigma_{Th}^{e} \quad , \qquad (4)$$

where

$\varepsilon = E \frac{E^{\gamma}}{m_e c^2}$ is the reduced photon energy,

and $\sigma_{Th}^{e} = 6.65 \cdot 10^{-25} cm^{2}$ is the Thompson cross section for elastic scattering of photons on electrons. In addition to the kicked out electron, a characteristic X-ray or Auger electron can also appear. The Auger electrons usually have much lower energy than the primary photoelectron and are of no interest.

The Compton effect describes the interaction of photons and quasi-free atomic electrons. Eq. 5 gives the energy dependence of the scattered photon.

$$h\nu' = \frac{h\nu}{1 + \frac{h\nu}{m_e c^2}(1 - \cos\theta)} \qquad (5)$$

The angular distribution is given by the Klein-Nishina formula [7,10] and is shown in Fig. 3. The higher energy of the incident photon corresponds to forward scattering, while at low energies, backscattering is also highly probable.

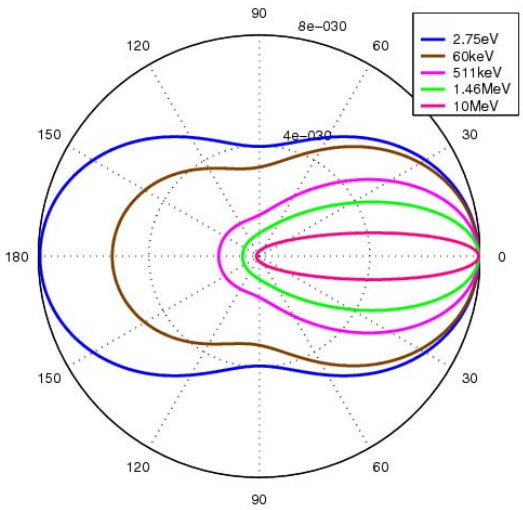

Figure 3: Angular distribution of scattered photons [11].

Pair production takes place in the Coulomb field of a nucleus. It becomes possible when photon's energy is higher than $2m_ec^2$ [8].

Considering that the incident photon disappears in one of three processes, the number of photons penetrating a thickness *z* of material is described by exponential decay.

$$I(z) = I_0 e^{-\mu z} \quad , \qquad (6)$$

where μ is the total attenuation coefficient of all three processes [9]. It is common practice to measure the thickness in g/cm^2, which is simply the linear thickness multiplied by material density. Fig. 4 shows a typical cross section's dependence on the photon's energy.

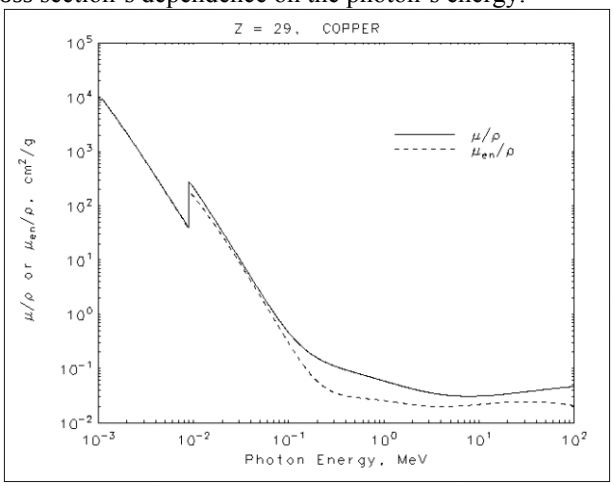

Figure 4: Energy dependence of attenuation coefficient [41].

Nuclear interactions

High energy hadrons interact with the nucleus. Different models could be used to describe such interactions. Just to name a few:

- Evaporation [12,13].
- Multifragmenation [14].
- Fermi breakup [15].
- Low energy neutron interactions [16].
- Cascading [17].

For hadron accelerators, the processes of great interest are evaporation and low energy neutron transport. The first process is the main source of neutrons in hadron machines, and the second one describes neutron propagation in accelerator materials and detectors.

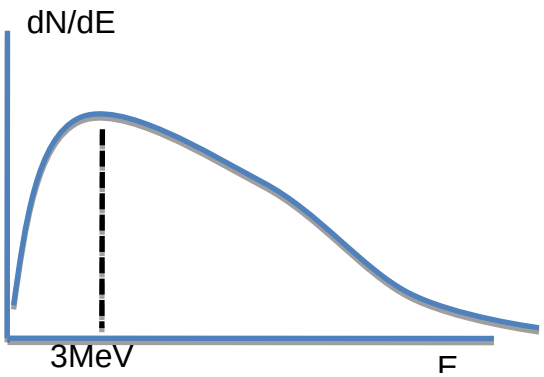

Figure 5: Energy spectrum of evaporation neutrons.

The evaporated neutrons have an average energy of 3 MeV but the spectrum extends up to 20 MeV; a sketch is shown in Fig. 5. A typical scenario of neutron generation includes cascade development, evaporation of neutrons (and other hadrons), and their further propagation.

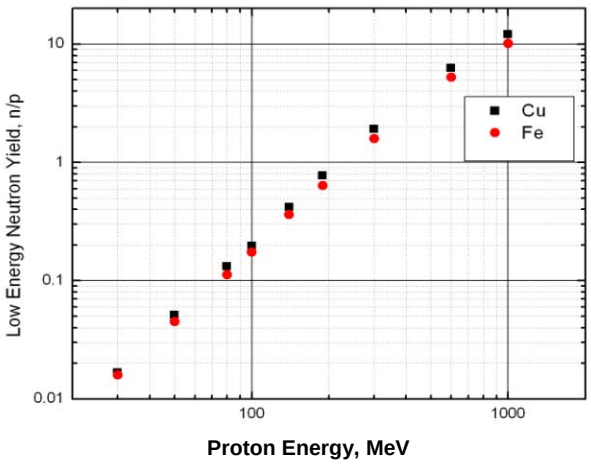

Figure 6: Evaporation neutron yield from a copper target as a function of incident proton energy [18].

The cross sections for low energy neutron interactions are contained in well-known tabulated data. Figures 7-9 contain cross-sections of different interaction types in different materials [19].

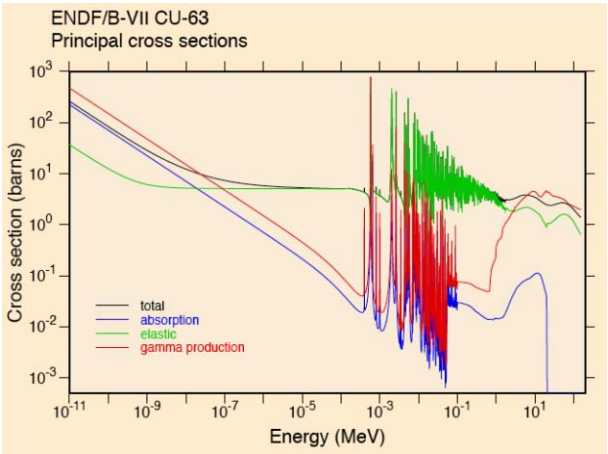

Figure 7: Neutron scattering on copper.

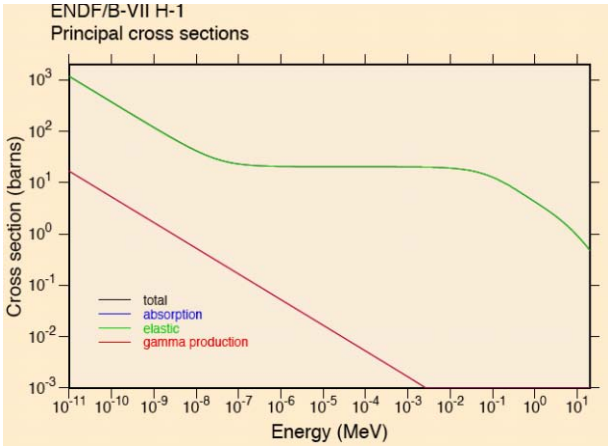

Figure 8: Neutron scattering on hydrogen. The high elastic cross section makes hydrogen the most efficient neutron moderator.

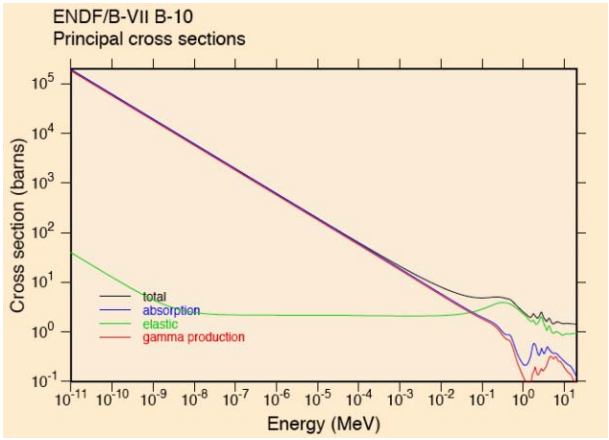

Figure 9: Neutron scattering on boron. High absorption cross section allows boron's use for neutron detection.

Radioactivity

Radioactivity is not directly related to beam loss, but is considered in order to limit residual activation of accelerator elements and surroundings. Also, the residual activation itself is a valuable source of information about beam loss. If the gamma spectrum is measured, one can try to find out what isotopes are producing it, then further estimate this particular isotope production, and finally, estimate beam loss that could cause such production.

Radioactivity is the random process of nucleus disintegration. The number of isotopes decreases exponentially with time (Eq. 7):

$$N(t) = N_0 e^{-\lambda \cdot t} \quad . \tag{7}$$

Historically the isotopes are characterized by the half-life (period after which half the radioactive isotope has undergone decay).

Radiation units [20]

Many radiation units exist, and such a multiplicity often leads to confusion. A loss monitor's signal is usually proportional to energy deposited by radiation in the sensitive volume of the detector or to particle flux inside it. Thus the main unit of interest is the gray (Gy), which is 1 joule of deposited energy per kilogram. Rad is also used; 1 rad = 0.01 Gy.

If a signal is proportional to particle flux, then flux units are used, for example, $1/cm^2/s$ (number of particles per unit area per second).

The other units, less important for BLMs, are:

- Sievert (Sv), a Gy multiplied by a quality factor for biological impact.
- REM or Röntgen Equivalent in Man; 1 REM=0.001 Sv (obsolete unit).
- Curie (Ci); 1 Ci=3.7×10^{10} disintegrations per second.

LOSS MONITOR TYPES

A great variety of loss monitor types exists. We will talk about ionization chambers, scintillators, PIN diodes, secondary emission monitors, and, briefly, Cherenkov light detectors. We will follow an excellent overview given in [21].

Ionization Chamber

An ionization chamber is filled with gas and has a high voltage bias applied to electrodes. The chambers can have different shapes but usually are coaxial cylinders.

Figure 9: SNS ionization chamber. Contents = 113 cm^3 of argon; HV= –1000V; sensitivity 70 nC/rad.

The radiation ionizes gas inside the chamber and the resulting charge is collected by electrodes. The shape of the electrode defines the time characteristics, while the sensitivity depends on the total volume of the chamber. Depending on high voltage (HV), the ion chamber can operate in different modes as shown in Fig. 10. When HV is low, a recombination process takes place before the ions and electrons are actually collected by the electrodes. Increasing the HV brings the chamber into ionization mode when all charge is completely collected. Further increase of the HV leads to the proportional mode, when the ions create secondary ionization and an avalanche.

The most typical mode is ionization because the chamber sensitivity stays the same for fluctuating HV.

The common gases used for ion chambers are argon and nitrogen, but air will work as well. The HV ranges from several hundred V to several kV.

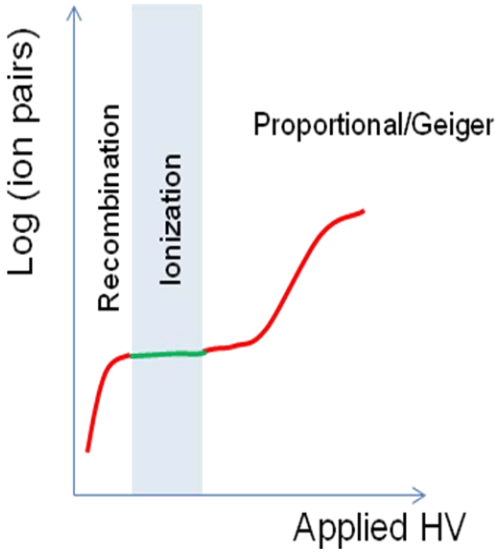

Figure 10: Different modes of ionization chambers.

If time resolution is important, the geometry should be optimized to improve the response time of the ion chamber. The response time of the SNS ion chamber is around 1-2 μs [21]. From the signal side, the ion chamber is a current source, so a transimpedance amplifier is used for analog front end electronics.

The main advantages of ionization chambers include:

- Calibration determined by geometry (no HV dependence).
- No maintenance (even a leaking nitrogen chamber continues to work in air).
- Radiation hard (10^8 rad).

Currently, ion chambers are the main type of loss monitor type used in hadron machines (SNS, LHC, RHIC, Tevatron).

There is also a variation of ion chamber in which the detector is very long (3 m or even longer). An example is shown in Figure 11.

Figure 11: Long ion chamber at ISIS [22].

Solid state Ion Chamber – PIN photodiode

The same principle of charge creation is used in semiconductors. The radiation creates electron-hole pairs and the charge is collected by biased plates as in Fig. 12.

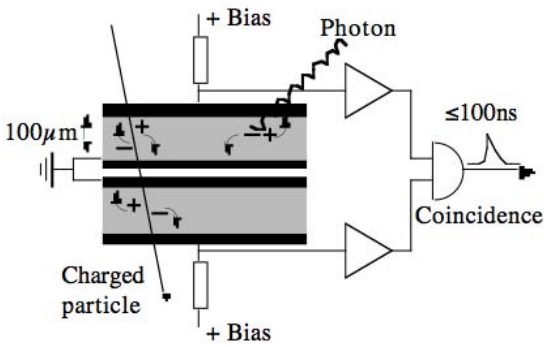

Figure 12: PIN diode schematics in coincidence mode [21,23].

The PIN diode is much faster than the ion chamber, with a response time of about 5 ns. While it can be used in waveform mode, counter mode is more common. The combination of two PIN diodes makes a loss monitor insensitive to gamma radiation (because gammas produce signal in one detector diode only).

Scintillator based detectors

The scintillator based detectors are probably the second most popular for beam loss monitoring, after ion chambers. The scintillation itself is a molecular effect. The fluorescent material emits UV light in response to energy deposited by a particle. This light is in turn absorbed by a material that emits visible light. The visible light is detected by a photocathode. One has to match the wavelengths of these two materials and also match the photocathode sensitivity. A vast review of scintillators is given in [24].

Usually scintillating materials are dissolved in plastics or liquid so it is possible to obtain almost arbitrary shapes. Figs. 12 and 13 show different scintillator based detectors.

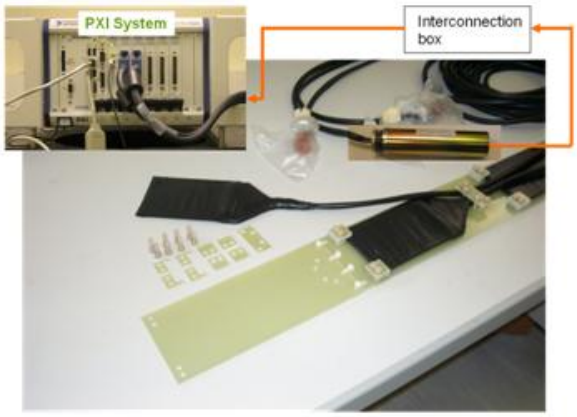

Figure 12: Scintillator detector at ISIS [22].

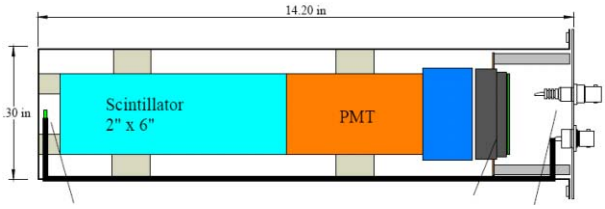

Figure 13: Fast loss monitor at SNS.

The scintillators are usually used with photo-multiplier tubes. This gives a typical signal gain of 10^5–10^8 which can be regulated by the applied HV. This gain is achieved in the accelerator tunnel, which simplifies further signal conditioning (in the case of the ion chamber there is no pre-amplification). See Fig 13.

Modification of the scintillator material can effectively change its sensitivity to different types of radiation. SNS neutron detectors use a scintillator doped with LiFxZnS(Ag) and slow neutrons are detected by means of the ^{6}Li(n,alpha) reaction. In this case, the scintillator detects secondary alphas from this reaction)[18].

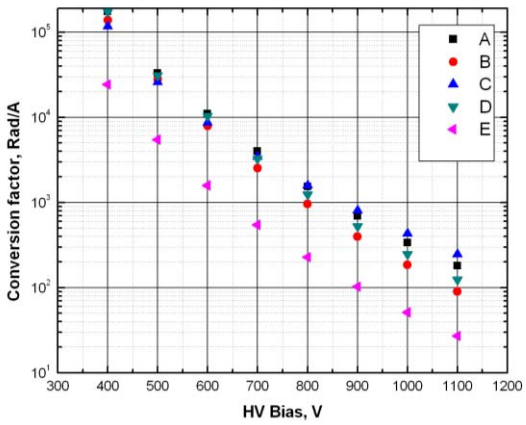

Figure 13: Sensitivity dependence of SNS scintillator-based neutron detectors on HV[18]

Scintillator-based detectors are easy to test with a built-in LED. They have fast response (20-100 ns), and more important, the response time spread is around 1–5 ns.

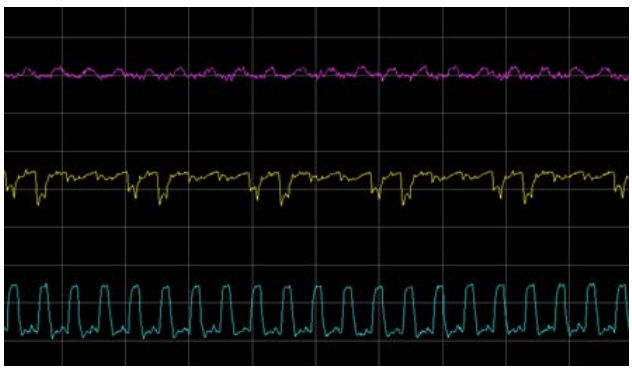

Figure 15: Scope screenshot (2 μs/div) of fast loss monitor at SNS. Detector resolves the ~700 ns mini-pulse structure of the SNS linac.

If a PMT-based detector is used in waveform mode, it effectively represents a current source similarly to an ion chamber. Both detectors require HV of the same scale, so it is often quite easy to use the same set of cables/electronics for both types of detectors.

Scintillators have the big disadvantage of being not being extremely radiation tolerant (~100 kGy decreases sensitivity by factor of 2, but numbers vary greatly depending on scintillator type). The transparency degrades with exposure, making calibration difficult.

Secondary Emission Monitor

The secondary emission monitor (SEM) is somewhat different than detectors discussed earlier. It exploits secondary emission from the surface caused by particles crossing this surface (the detectors discussed above use volume rather than surface as the main sensitive part). Understanding the principles of operation requires solid state physics knowledge. A good introduction to the theory of secondary emission regarding loss monitoring is given in [26].

The secondary yield depends on incident energy according to the Sternglass formula; [25] see Fig. 16.

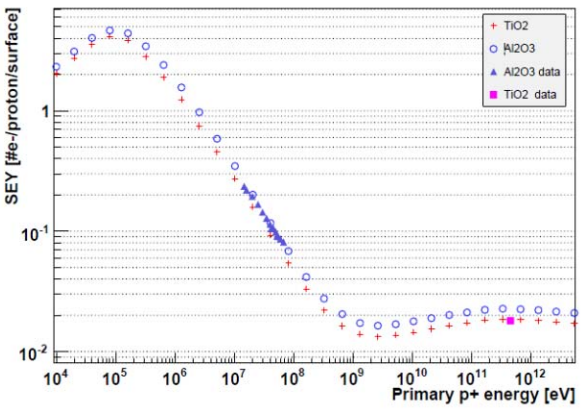

Figure 16: Secondary electron yield per incident proton [26].

The SEMs are very radiation hard and have low sensitivity (see Table 1). It makes sense to put them into high radiation areas where other detectors would be saturated or damaged by radiation. The LHC uses a combination of ionization chambers and SEMs [26].

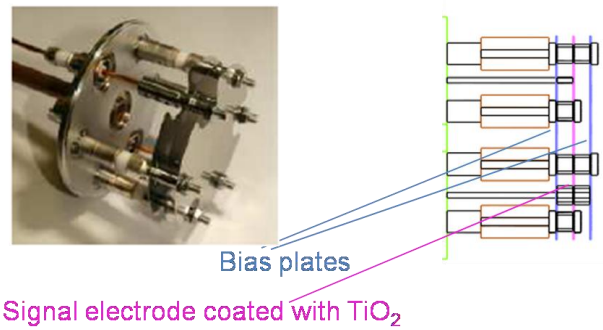

Figure 17: Large Hadron Collider SEM [26].

Cherenkov light detector

When an electron travels in a medium faster than the speed of light in that medium, the medium itself radiates photons. Photon yield is described by

$$\frac{dN}{dx} = 2\pi\alpha \sin^2\Theta \cdot \left(\frac{1}{\lambda_1} - \frac{1}{\lambda_2}\right) \quad , \qquad (8)$$

where $\cos(\Theta) = \frac{1}{\beta_n}$, $\alpha = \frac{1}{137}$, and $\lambda_{1,2}$ is the wavelength interval.

Considering photocathode sensitivity, we are interested in a 350-500 nm interval, which gives [21]

$$\frac{dN}{dx} = 390 \sin^2\Theta \cdot \frac{photons}{cm} \quad . \qquad (9)$$

Cherenkov detectors are widely use in light sources. The configuration of the detector is very specific to the accelerator, accounting for electron energy and geometrical factors.

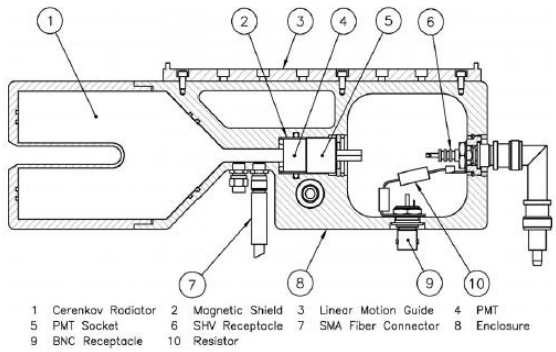

Figure 18: Cherenkov detector at the Linac Coherent Light Source (LCLS) [27].

Other types of detectors

We don't include a detailed discussion of diamonds and fibers in this paper. Diamond detectors are relatively new and not widely used in accelerators, but are quite promising, with high dynamic range, high sensitivity, and radiation hardness [28]. Fiber detectors could be effectively used to determine loss location using the optical transition radiation (OTR) technique [21].

Avalanche diodes [29] can substitute for PMTs in some situations. They are compact and insensitive to magnetic field, but they require very stable temperature and voltage control, and they respond to direct radiation much more strongly than to the light emitted by scintillator. There was an attempt at using avalanche diodes coupled to scintillating fiber at SNS. No significant advantage over PMTs was achieved.

Loss monitor selection

It is hard to come up with a common recipe for loss monitor selection, since the choice will strongly depend on accelerator specifics. Here are generic things to consider:

- Sensitivity and dynamic range.
- Analog output or counter. This choice can significantly affect the system design, so it has to be done very carefully.
- Radiation hardness. The type of radiation is also very important for scintillators and PIN diodes. The "light" radiation (electrons and gammas) usually causes less damage.
- Calibration importance. If absolute values are required, then calibration should be simple or unnecessary (ion chambers).
- Test procedure complexity (an LED could be used for scintillators, but not for ion chambers).
- Time resolution. If beam pulse structure should be resolved, ion chambers are ruled out.
- Reliability.
- Complexity of electronics. An ion chamber will require electronics of large dynamic range; the gain of PMT-based detectors can be adjusted with HV.
- Size and cost. Depending on the goals, the required size could be from several millimeters up to several meters and sometime higher.

Some loss monitor parameters are summarized in Table 1 [21].

Table 1: Sensitivity for different loss monitors.

Detector	Energy to create one e^- [e^-/eV]	Sensitivity [nC/rad]
Plastic scintillator (1 ltr)	250-2500	10^4 $Gain_{PMT}$
Inorganic scintillator (1 ltr)	50-250	10^5 $Gain_{PMT}$
Ion chamber (1 ltr)	22-95	500
PIN diode 1cm^2	3.6	50
SEM (8 cm^2)	2-5% (dE/dx)	10^{-3} $Gain_{PMT}$
Cherenkov light (1 ltr)	10^5-10^6	270 $Gain_{PMT}$

As rough guidance for high intensity hadron accelerators, we would suggest: ion chambers for machine protection; scintillators for good time resolution and changing gain with HV; and SEMs for high radiation areas. For electron machines, the list would be: PIN diodes as a low cost solution and no sensitivity to gammas; Cherenkov detectors; and scintillators.

BEAM LOSS SIMULATION

Ideal BLM system

While no ideal system exists, it is useful to formulate the main features of such a hypothetical system:

- Radiation detector with high dynamic range to be used for both regular (low) loss and irregular (high and fast) loss.
- Sensitive only to radiation caused by beam loss.
- Allows one to find out the amount of beam lost (conversion from radiation intensity to actual number of primary particles).
- Resolves time structure of loss.
- Resolves spatial distribution of beam loss.

Consider the simplified system that accounts for only one type of secondary particle as sketched in Fig. 19.

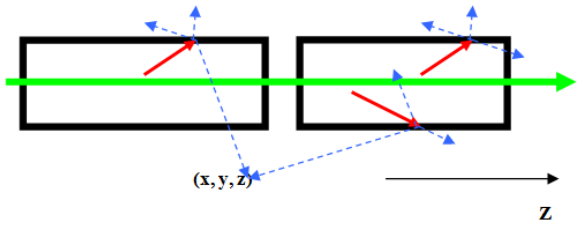

Figure 19: Sketch of beam loss process.

$$N_0 = \iiint N(X,Y,Z)\,dXdYdZ \qquad (10)$$

$$L(x,y,z) = \iiint N(X,Y,Z)P(x,y,z,X,Y,Z)\,dXdYdZ \qquad (11)$$

$$Ld = \int L(e,x,y,z)S_d(e)\,de \qquad (12)$$

where N_0 is the total number of lost particles, $N(X,Y,Z)$ is the spatial density of lost particles, $P(e,x,y,z,X,Y,Z)$ is the probability of secondary particles having energy e reaching position (x,y,z), L is the number of secondary particles in (x,y,z), L_d is the BLM signal, and S_d is the detector response function. To effectively determine $L(x,y,z)$, a computer simulation is used.

The ultimate goal of a BLM system is to solve Eq. (11) and find $N(X,Y,Z)$. Even in the case of an infinite number of ideal BLMs, the solution of (11) could be non-unique. Of course we don't have an infinite number of detectors, so even the measurement of $L(x,y,z)$ presents a challenge.

Figs. 20 and 21 demonstrate that the choice of BLM can significantly change the measured loss pattern. The same losses in the SNS [18] warm linac are measured by different types of detectors: ionization chambers and neutron detectors. The losses are caused by insertion of different Faraday cups. The Faraday cups are installed between Drift Tube Linac (DTL) tanks where beam energy is 7.5 MeV (FC1) to 72.5 MeV (FC5). BLMs are numbered from 1 (installed at ~3 MeV) to 20 (~90 MeV). The ionization chambers respond to nearby loss and thus are able to resolve loss location, but they will be insensitive to loss occurring between two detectors. Conversely, the neutron detectors respond to any loss, close or remote, and are effectively covering a wider region, but are incapable of spatial resolution.

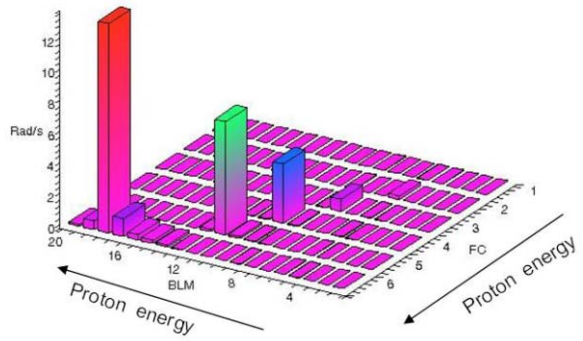

Figure 20: Losses measured by ionization chambers [18].

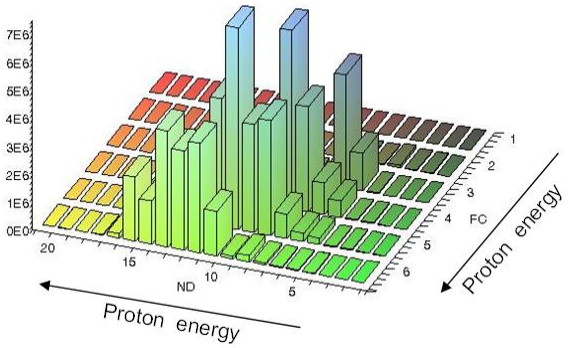

Figure 21: Losses measured by neutron detectors [18].

This is explained by a neutron's ability to penetrate beam pipes (the main materials are copper and steel, which don't attenuate neutrons effectively), whereas ionization chambers detect mainly gammas, which are effectively attenuated by these materials.

Monte Carlo codes

The standard way of simulating radiation propagation in a medium is to employ Monte Carlo codes. Modern codes include vast physics models and capabilities to simulate realistic beam line geometries.

Among most widely used codes are:

- MCNPX (LANL/ORNL) [30].
- MARS (FNAL) [31].
- GEANT4 (CERN/SLAC and others) [32].
- FLUKA (CERN/INFN) [33].
- SHIELD (INR), for hadrons only [34].

A typical simulation would contain stages (each stage using the code that is good for that particular stage) as shown in Fig. 22. It includes loss simulation of primaries by some beam dynamics code (e.g., PARMILA [35]), and then generation of secondaries and their transport in a medium.

While all these codes have some advantages and disadvantages, we will describe GEANT4 as the code that is most flexible for modification and applicable in most situations.

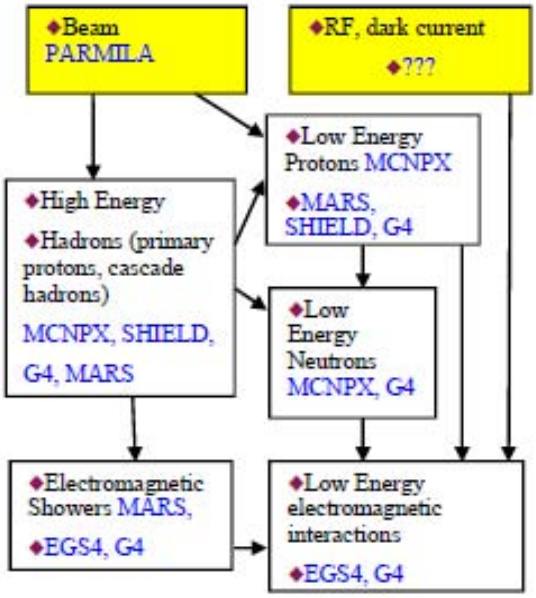

Figure 22: Applicability of different Monte Carlo codes to loss simulation.

GEANT4

The very important difference between GEANT4 (G4) and other simulation codes is that it is not a final, user-ready program but a toolkit. It is written in C++ while almost all others are FORTRAN. The use of Object Oriented Design allows effective decoupling of different physics models and other modules. To understand or modify an existing physics model, one need only examine the piece of code responsible for this particular type of interaction. This allows user to apply expertise in a narrow specific field without danger of influencing the other parts of the code, where default models could be used. Different statistical techniques (such as event biasing or Russian roulette) can be easily added as needed. Deep granularity of physics processes makes possible to apply different models to the particles at different energies and in different geometrical locations.

Usually the process of geometry definition is difficult and tedious, since different codes use different input formats that are not always compatible. G4 allows importation of CAD system files, so one can concentrate on physics processes rather than on geometrical assumptions and configuration. It has powerful visualization tools and its quality is comparable to CAD visualization.

Like all other Monte Carlo codes, G4 is easily parallelizable, and performance per CPU stays almost constant with an increasing number of CPUs.

G4 contains different physics models, and the user can define which one to use. The electromagnetic interactions include:

Photon processes

- γ conversion into $e^+ e^-$ pair
- Compton scattering
- Photoelectric effect
- Rayleigh scattering
- Gamma-nuclear interaction in hadronic sub-package

Electron and positron processes

- Ionization
- Coulomb scattering
- Bremsstrahlung
- Nuclear interaction in hadronic sub-package
- Positron annihilation

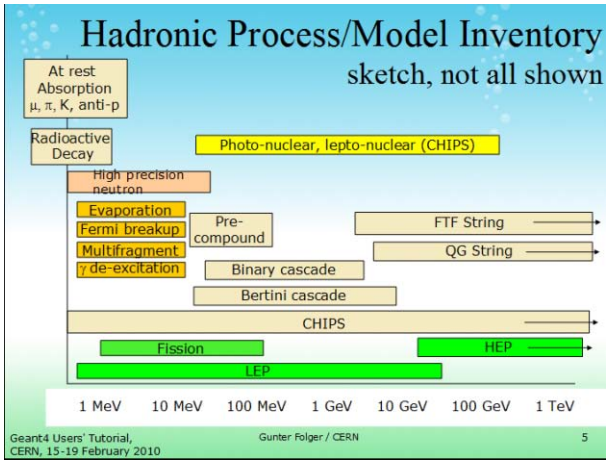

Figure 23: Hadronic models in G4 [36].

One of the possible extensions of G4 physics is described in [26] where a model of secondary electron emission is added to standard G4 to simulate SEM loss monitors at LHC.

Common use cases

The simulations are frequently used for calculations of thresholds for machine protection [37]. This is a straightforward simulation when the loss rate is limited by equipment specifics and the BLM response signal is simulated for the maximum allowable loss rate.

The other quite common application is obtaining knowledge about the loss monitor detector itself, i.e., calculating the detector response function L_d. A rigorous investigation was done by the LHC team to build detector response functions for their BLMs[37].

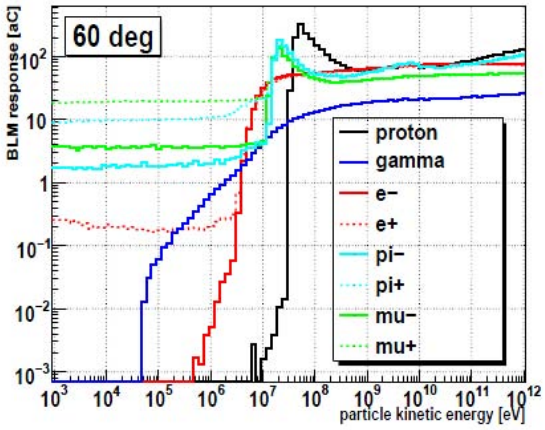

Figure 24: LHC BLM response function [37].

A good way to benchmark simulations is to create intentional loss and measure the BLM's response. The response of neutron detectors to insertion of Faraday cups (Fig. 25) was simulated with the code SHIELD.

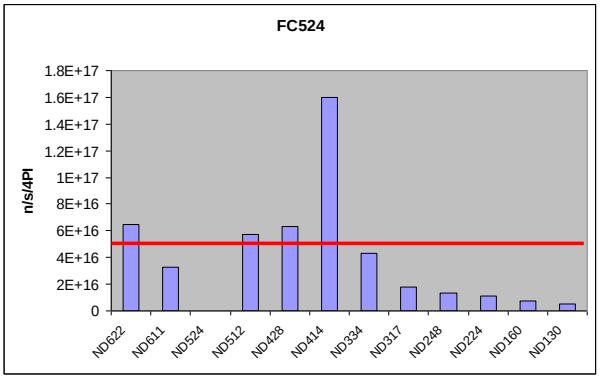

Figure. 25: Neutron detector measurements (blue bars) vs. simulation (red line) [18].

Fig. 25 demonstrates that ND414 was not calibrated correctly and that either the angular distribution is incorrect in the model or the geometrical assumptions are poor (remote detectors in a backward direction show lower signal than the measurement).

Proposed loss simulation for new machine

As previously mentioned, it is now possible to import CAD geometry into the simulation program. Therefore, it would be beneficial to have the whole machine designed in one CAD package. The process of loss simulation could be briefly described with the following steps.

The machine setup (geometry/materials/fields) should be imported into G4. Machine specific loss physics has to be researched:

- Perform benchmarking of G4 with other codes (MCNPX, FLUKA, MARS) for physics models of interest for several primitive geometry test cases.
- Compare simulation data with experiment.
- Rule out discrepancies.
- Modify G4 physics.

The most probable loss locations can be obtained from accelerator physics specialists, and corresponding loss scenarios should be simulated to obtain a feeling for the loss pattern and scale. This will allow determination of a detector candidate.

The list of loss sensitive equipment should be collected as soon as possible and the maximum admissible losses simulated. This will give the prediction of threshold levels and offer detector candidates dedicated to machine protection.

Considering the BLMs as tuning devices will probably result in a completely different list of requirements and will lead to different detector candidates.

Additional tasks: Try to build a model of an ideal detector that will satisfy all requirements. Perform simulation of the ideal detector's response to insertable devices. Perform "scan" simulations (for different point losses along the machine) of the whole accelerator and build the function P(x,y,z,X,Y,Z) from (11).

While it seems to be very hard to implement, it is quite possible with current computing power, and will be easier in the future. This procedure reverses the common process in which existing designs are simulated—it actually allows simulations to drive the design.

MACHINE PROTECTION SYSTEM (MPS)

Almost all high power/high energy machines use BLMs in a protection mechanism that inhibits the beam if loss exceeds some threshold. It is extremely important in hadron machines. We will compare the MPS systems of SNS [38] and LHC [39,40] to demonstrate the evolution during the last two decades.

The SNS BLM protection system is an "old school" analog-based design where the loss signals from ~350 BLMs are integrated by analog integrators and afterwards compared with a DAC level representing the maximum permissible loss level. The detector signals (current from ionization chambers or PMTs) are brought from the accelerator tunnel, then amplified in the Analog Front End (AFE), and then split into three signals to be fed into the digitizer and integrator. The leaky integrator discharges itself before the next pulse comes (in 16 ms).

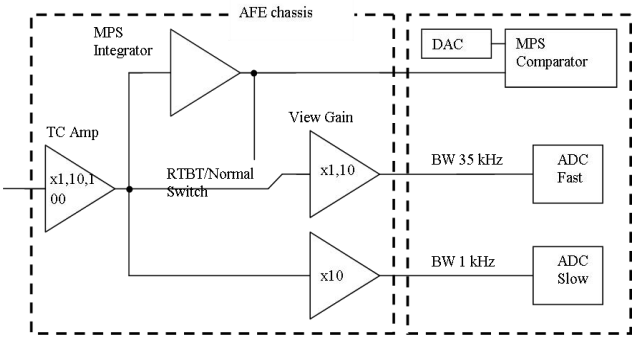

Figure 26: SNS AFE schematics.

The comparator interlocks the beam within 15 microseconds after the integrated signal exceeds the threshold. In addition to this fast hardware-based limit, a slow 1 second limit is calculated in software. In this way, SNS has two limits per BLM. One is purely hardware-based and the second one is software-based.

The LHC MPS system [39] consists of more than 3500 BLMs and uses an FPGA-based design. The analog current signal is converted into a frequency signal and 40 microsecond sum, which is pushed into an FPGA. Several running sums are calculated (with time windows from 40 microseconds to several seconds).

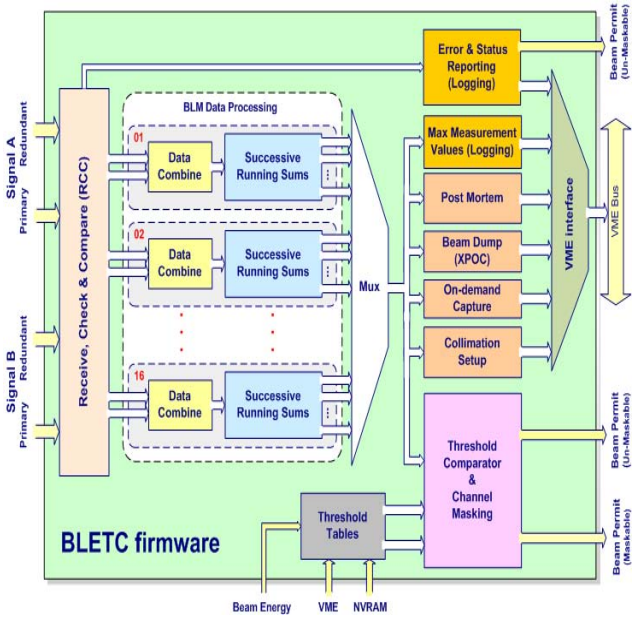

Figure 27: The schematic of LHC MPS [40].

The limits depend on beam energy so every BLM effectively has a two-dimensional array of limits. All limits are calculated by the FPGA.

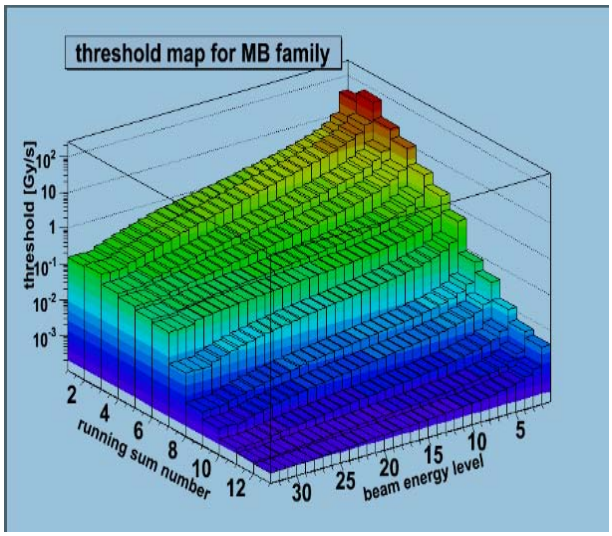

Figure 28: Two-dimensional array of limits for LHC BLM [39].

The functionality of hardware-based and software-based interlocking is merged into an FPGA, introducing much higher degree of flexibility. Table 2 summarizes these two approaches.

Table 2: Analog vs FPGA based MPS design

	Analog (SNS)	**FPGA (LHC)**
Analog FE	Outside of the tunnel (current signal over long cables)	In the tunnel, digital link to controlling FPGA
Integration	Hardware integration one window (16mS leaky integrator)	FPGA digital integration many windows
Additional Integration	Software integral over 1 second	N/A
Limits	Set by software, reinitialized every IOC reboot	Limits set in software and loaded into non-volatile memory in FPGA
Timing System	Independent	Independent
Preamplifier Gain	Jumper settings	N/A
Reliability	Analog component	Complex FPGA code verification procedure
HV distribution	Daisy chained 1-4 BLMs with HV current/HV voltage monitoring in software. Next generation system will have a dedicated PS per BLM.	Daisy chained over 400-600 BLMs with 2 redundant HVPS, FPGA monitoring of HV health

CONCLUSIONS

There are many ways to detect beam losses, but no single best way because every machine is different. Ion chambers remain the most widely used detectors, especially among hadron machines. The new advances in materials improve loss monitor characteristics, but the underlying physics principles are the same—usually it is ionization loss Eq. (1-2).

Computer simulations are widely used in BLM design, and it will probably step up to the next level in the nearest future.

The electronics used to interface BLMs to the machine protection system changed significantly with availability of FPGAs.

ACKNOWLEDGEMENT

ORNL/SNS is managed by UT-Battelle, LLC, under contract DE-AC05-00OR22725 for the U.S. Department of Energy.

REFERENCES

Three books are extensively cited in this paper. *Particle Detectors* [3] and *Radiation Detection and Measurement* [2] give brilliant overviews of detectors and detector principles. *An Introduction to the Passage of Energetic Particles through Matter* [1] thoroughly discusses different physics processes and contains compilation of many data sources regarding cross-section and other experimental data.

[1] N.J. Carron , *An Introduction to the Passage of Energetic Particles through Matter*, Taylor & Francis, 2007.
[2] G. Knoll, *Radiation Detection and Measurement*, third edition, John Wiley & Sons, 2000.
[3] G. Grupen, B.A. Shwartz, *Particle Detectors*, second edition, Cambridge University Press, 2008.
[4] Ibid, pp. 2-11.
[5] M.J. Berger et al "Stopping-Power and Range Tables for Electrons, Protons, and Helium Ions", NIST, http://www.nist.gov/physlab/data/star/index.cfm.
[6] G. Grupen, B.A. Shwartz, *Particle Detectors*, 2nd ed., Cambridge University Press, 2008, pp. 32-33.
[7] Ibid, pp. 34-35.
[8] Ibid, pp. 36-37.
[9] Ibid, pp. 38-41.
[10] Klein, O; Nishina, Y (1929). Z. f. Phys. **52**: 853 and 869.
[11] http://en.wikipedia.org/wiki/Klein%E2%80%93Nishina_formula.
[12] V. E. Weisskopf and D. H. Ewing. Phys. Rev. **57**, 472 (1940).
[13] I. Frenkel, Sov. Phys. **9**, 533 (1936).
[14] J.P. Bondorf, A. S. Botvina, A.S. Iljinov, I.N. Mishustin , K. Sneppen., Physics. Reports. **257**, 133 (1995).
[15] E. Fermi, Prog. Theor. Phys. **5**, 1570 (1950).
[16] ENDF/B-VI: Cross Section Evaluation Working Group, ENDF/B-VI Summary Document, Report BNL-NCS-17541 (ENDF-201) (1991), edited by P.F. Rose, National Nuclear Data Center, Brookhaven National Laboratory, Upton, NY, USA.
[17] M. P. Guthrie, R. G. Alsmiller and H. W. Bertini, Nucl. Instr. Meth. **66** (1968), 29.
[18] A. Zhukov, S.Assadi "Beam Loss Simulation of SNS LINAC", FRPMN060, in Proceedings of the Particle Accelerator Conference (PAC 07), Albuquerque, New Mexico, 25-29 Jun 2007, p. 4138.
[19] ENDF/B-VII Incident-Neutron Data, http://t2.lanl.gov/data/neutron7.html.
[20] G. Grupen, B.A. Shwartz, *Particle Detectors*, 2nd ed., Cambridge University Press, 2008, pp. 71-76.
[21] K. Wittenburg, "Beam Loss Monitors", CERN Accelerator School 2008, http://cas.web.cern.ch/cas/France-2008/Lectures/Wittenburg-BLM.pdf.
[22] D.J. Payne et al, "Beam Diagnostics at ISIS", Workshop on High Intensity, High-Brightness Hadron Beams, August 25-29, 2008 http://ics-web4.sns.ornl.gov/hb08/WGF10.PDF,
[23] J. Bergoz, personal communication.
[24] G. Knoll, *Radiation Detection and Measurement*, third edition, John Wiley & Sons, 2000, pp. 219-265.
[25] E.J. Sternglass, Theory of Secondary Electron Emission by High-Speed Ions, Phys.Rev. 108(1957)1.
[26] D. Kramer, "Design and Implementation of a Detector for High Flux Mixed Radiation Fields", PhD thesis, http://ab-div-bdi-bl-blm.web.cern.ch/ab-div-bdi-bl-blm/Talks_and_papers/Kramer/thesis_DKramer.pdf.
[27] W. Berg et al., "Development of a Beam Loss Monitor System for the LCLS Undulator Beamline", TUP043, in Proceedings of LINAC08, Victoria, BC, Canada,http://epaper.kek.jp/LINAC08/papers/tup043.pdf.
[28] E. Griesmayer, "Diamond Detectors as Beam Monitors", these Proceedings.
[29] G. Knoll, *Radiation Detection and Measurement*, third edition, John Wiley & Sons, 2000, pp. 287-292.
[30] MCNPX, Version 26E, LA-UR-07-6632 2007, https://mcnpx.lanl.gov/opendocs/versions/v26e/v26e.pdf.
[31] N.V. Mokhov, S.I. Striganov, "MARS15 Overview", Fermilab-Conf-07/008-AD (2007), in Proc. of Hadronic Shower Simulation Workshop, Fermilab, September 2006, AIP Conf. Proc. 896 (2007) 50-60.
[32] J.Apostolakis et al., "Geometry and physics of the Geant4 toolkit for high and medium energy applications", Radiation Physics and Chemistry **78** (2009), 859-873.
[33] F. Ballarini et al., "Nuclear models in FLUKA: present capabilities, open problems and future improvements" ND2004, Santa Fe, 26 Sep - 1 Oct 2004, SLAC-PUB-10813.
[34] N.M.Sobolevsky, "The SHIELD Transport Code: a Tool for Computer Study of Interaction of Particles and Nuclei with Complex Media," in Proceedings of the 3rd Yugoslav Nuclear Society International Conference (YUNSC 2000), Belgrade, October 2-5, 2000. The VINCA Institute, Belgrade, 2001, p. 539.
[35] Phase and Radial Motion in Ion Linear Accelerators (PARMILA), http://laacg.lanl.gov/laacg/services/download_PMI.phtml.
[36] Geant4 Users' Tutorial, CERN, Feb. 15-19, 2010 http://indico.cern.ch/conferenceDisplay.py?confId=58317.
[37] M. Stockner, "Beam Loss Calibration Studies for High Energy Proton Accelerators", thesis http://cdsweb.cern.ch/record/1144077/files/CERN-THESIS-2008-099.pdf.
[38] Witkover, R. L. and Gassner, D., "Preliminary Design of the SNS Beam Loss Monitoring System", BIW2002, AIP Conf Proc 648 (2002).
[39] B. Dehning et al., "First Experience with the LHC Beam Loss Monitoring System", CERN-ATS-2009-025, pesented at the Particle Accelerator Conference (PAC09) May 4-8 2009, Vancouver, Canada.
[40] C. Zamantzas, "Reliability Tests of the LHC Beam Loss Monitoring FPGA Firmware", TUPSM089, these proceedings.
[41] C.T. Chantler et al "Detailed Tabulation of Atomic Form Factors, Photoelectric Absorption and Scattering Cross Section, and Mass Attenuation Coefficients for Z = 1-92 from E = 1-10 eV to E = 0.4-1.0 MeV", NIST, http://www.nist.gov/physlab/data/ffast/index.cfm